

## Analysis of the state of poling of lead zirconate titanate (PZT) particles in a Zn-ionomer composite

Nijesh Kunnamkuzhakkal James<sup>a</sup>, Tim Comyn<sup>b</sup>, David Hall<sup>c</sup>, Laurent Daniel<sup>c</sup>, Annette Kleppe<sup>d</sup>, Sybrand Van Der Zwaag<sup>a</sup>, and Wilhelm Albert Groen<sup>a,e</sup>

<sup>a</sup>Novel Aerospace Materials Group, Faculty of Aerospace Engineering, Delft University of Technology, Delft, The Netherlands; <sup>b</sup>Institute for Materials Research, University of Leeds, UK; <sup>c</sup>School of Materials, University of Manchester, Manchester, UK; <sup>d</sup>Diamond Light Source Ltd, Didcot, Oxfordshire UK; <sup>e</sup>Holst Centre, TNO, Eindhoven, The Netherlands

### ABSTRACT

The poling behaviour of tetragonal lead zirconate titanate (PZT) piezoelectric ceramic particles in a weakly conductive ionomer polymer matrix is investigated using high energy synchrotron X-ray diffraction analysis. The poling efficiency, crystallographic texture and lattice strain of the PZT particles inside the polymer matrix are determined and compared with the values for corresponding bulk ceramics reported in literature. The volume fraction of c-axis oriented domains and the lattice strain of the PZT particles are calculated from the changes in the integral intensities of the {200} peaks and the shift in the position of the {111} peaks respectively. It is shown that for an applied macroscopic field of 15 kV.mm<sup>-1</sup>, the PZT particles are effectively poled, leading to a maximum  $\nu(002)$  domain reorientation volume fraction, of around 0.70. It is also found that a significant tensile lattice strain,  $\epsilon_{\{111\}}$ , of 0.6% occurs in the direction of the applied electric field, indicating the occurrence of residual stresses within the 2–4  $\mu\text{m}$  size diameter particles. Although lower than that observed in poled tetragonal PZT ceramics, this level of lattice strain does indicate that the PZT particles within the composite experience significant elastic constraint. The correlation between the poling induced structural changes and the macroscopic piezoelectric and dielectric properties is discussed.

### ARTICLE HISTORY

Accepted 25 June 2015

### KEYWORDS

Piezoelectric composite;  
PZT; poling

## 1. Introduction

Lead zirconium titanate (PZT) ceramics exhibit high piezoelectric charge constant ( $d_{33}$ ), making them a suitable choice for actuators, but their high dielectric permittivity drastically reduces the voltage sensitivity for force sensing applications [1, 2]. On the other hand, piezoelectric polymers exhibit a high sensitivity ( $g_{33}$ ) but a much poorer actuator performance and this contrast in properties led to the development of piezoelectric composites, in which a piezoelectric ceramic material either in a granular or fibrous form is embedded in a polymeric matrix. This hybrid nature leads amongst others, to a lower density and the freedom to fine tune the acoustic impedance of transducers made out of such composites. As for

**CONTACT** Nijesh Kunnamkuzhakkal James  [nijeshkjames@gmail.com](mailto:nijeshkjames@gmail.com)

Color versions of one or more of the figures in the article can be found online at [www.tandfonline.com/gfer](http://www.tandfonline.com/gfer).

© 2016 Taylor & Francis Group, LLC

piezoceramics, piezoelectric composites need to be poled by applying a high dc electric field during a late stage of the manufacturing process. However, poling of such composites, in particular for the case of the piezoceramic particles all being surrounded by the continuous polymer matrix (so called 0–3 composites), is difficult since a large part of the externally applied electric field may be shielded by the polymer matrix having a low dielectric constant and a low electrical conductivity. As a result, very large electric fields are required to pole the ceramic fraction [3, 4]. Such large electric fields often cause dielectric breakdown of the composites. In addition, the presence of local weak points, such as pinholes or bubbles, short-circuits the electrodes and prevents thorough poling [5].

Recently we reported the attractive properties of PZT-ionomer composites, which include a decent value for the load sensitivity  $g_{33}$ , a high flexibility, good mechanical strength, excellent ceramic-polymer adhesion and a self-healing functionality [6]. The piezoelectric properties of ceramic-polymer composites depend on the poling state of the active PZT phase, as well as the dielectric properties of both phases and the type of connectivity present. The optimum poling conditions for soft PZT-ionomer composites were analysed by systematically studying the piezoelectric properties after poling under various conditions [6]. In that work, it was shown that the piezoelectric properties saturate at longer poling times, higher electric fields and elevated poling temperatures suggesting that the PZT phase is then relatively well poled. However, the actual state of poling of the particles in such composites have never been measured or compared to the state of poling in the fully dense ceramic reference state.

The electromechanical response in ferroelectric materials is comprised of both intrinsic (piezoelectric lattice strain) and extrinsic (domain wall motion) components. The non-180° domain switching and lattice strain that occurs during poling under an electric field above the coercive field can be determined from the changes in crystal structure as measured by X-ray diffraction has been reported in detail for bulk ceramics [7]. However, studies on PZT ceramics using conventional X-ray diffraction provide information only for the near-surface [8]. Guo et al. reported that the penetration depth in their study was in the region of 2  $\mu\text{m}$ , for an X-ray wavelength of 0.8 Å. The problems associated with studying the near surface region can be overcome by exploiting the intensity and penetration of high energy synchrotron X-rays, which is very much needed to probe the modified crystal structure of PZT particles in a polymer matrix due to poling [9].

The goal of this investigation is to further develop an approach to quantify the poling state of the PZT particles inside the polymer matrix by using high energy synchrotron X-ray diffraction. The results obtained from the diffraction experiment are correlated with the macroscopic property measurements.

## II. Experimental procedures

The piezoelectric ceramic powder used for manufacturing the composites was a *soft* PZT type (PZT507, Morgan Electroceramics, Ruabon, UK). In order to improve its piezoelectric properties the as-received powder was calcined at 1200°C for 2 h in a closed alumina crucible in a Nabertherm furnace applying a heating rate of 5°C/min. The calcined powder was ball milled using yttria stabilized zirconia balls of 5 mm diameter in cyclohexane for 4 hrs [10]. Subsequently, the powder was dried at 150°C and stored in a closed container to avoid moisture absorption. The average particle size ( $d_{50}$ ) of the milled powder is 4.3  $\mu\text{m}$  as measured by light scattering with a Horiba LA950DLA. The particle size measured with SEM

was about 3–5  $\mu\text{m}$ , which is in good agreement with the laser scattering results. Prior to making the composites, laboratory X-ray diffractometer (Bruker D8, Berlin, Germany) was used to identify the phases present in the PZT powder. The diffractometer uses  $\text{CoK}\alpha_1$  X-rays and the PZT powder was scanned with speed of  $2^\circ/\text{min}$ .

The polymer selected for the experiments is a commercial Zn-based ionomer (Surlyn 9320 DuPont), which is a partially ( $\text{Zn}^{2+}$ ) neutralized ethylene methacrylic acid copolymer. Apart from its excellent chemical resistance, good mechanical properties and its temperature stimulated self-healing capability, the ionomer has the desirable characteristic that the relaxation of the ionic species at elevated temperatures increases the electrical conductivity significantly, which should be beneficial to the poling efficiency. The electrical conductivity of the ionomer at the selected poling temperature of  $60^\circ\text{C}$  is  $3.96 \times 10^{-12} \text{ S/m}$ .

The composites were prepared by mixing polymeric matrix and PZT powder (30 volume%) in a lab-scale counter rotating twin screw extruder (DSM Xplore Research Netherlands). The processing temperature was kept at  $170^\circ\text{C}$ . In order to get a homogeneous distribution of PZT ceramic particles in the polymer matrix, the residence time was kept for 5 min, which ensured multiple passes of the material through the mixing section of the extruder. The composites were finally extruded through a 2 mm diameter outlet. In order to get planar sheets of composites, the extruded wire-shaped materials were hot pressed at a temperature of  $150^\circ\text{C}$  and a pressure of 1 MPa for 5 min, yielding flexible planar sheets with a thickness of about 1 mm. Electrodes on both sides of the samples were made by gold sputtering. The samples were poled in organic oil (rape seed oil) at an electric field of  $15 \text{ kVmm}^{-1}$  and a temperature of  $60^\circ\text{C}$  for 60 min.

The dielectric properties of the composites were measured using the parallel plate capacitor method using an Agilent 4263B LCR meter at 1 V AC signal and a frequency of 1 kHz. The  $d_{33}$  of the composites was measured using a Berlincourt-type  $d_{33}$  meter (KCF technology PM3001, State college, PA, USA). The P-E (polarisation-electric field) hysteresis loops of the composites were measured at room temperature using a Radiant hysteresis loop measurement system (RT 6000 HVS-2, Radiant Technologies Inc., Germany).

The synchrotron X-ray diffraction experiments were performed on Beamline I15 at the Diamond Light Source, UK. A schematic diagram of the high energy synchrotron X-ray diffraction experimental set up is shown in Fig. 1. A synchrotron X-ray beam with a cross-section of  $100 \times 100$  microns and a photon energy of 67 keV was used (wavelength =  $0.1839 \times 10^{-10}$

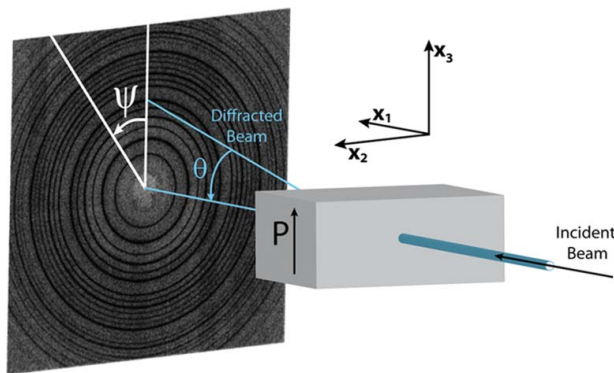


**Figure 1.** Experimental set up for time resolved high energy X-ray diffraction and the 2 D diffraction image shows the Debye-Scherrer rings.

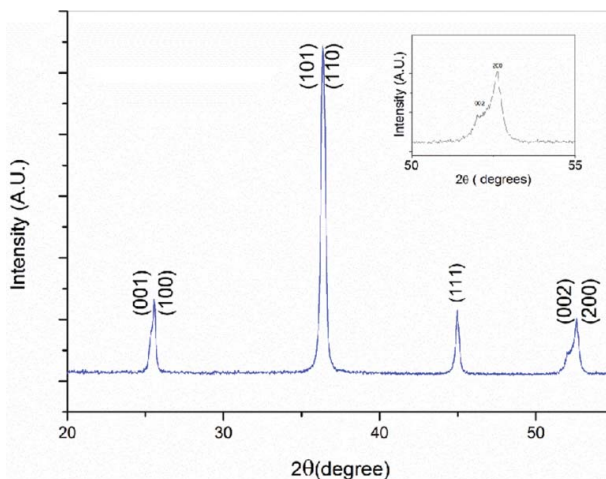


**Figure 2.** XRD diffraction pattern of PZT 507 powder used for fabrication of 0.3 ionomer composites.

m), with the diffraction patterns being recorded in transmission. A 2D detector (Perkin Elmer 1621 AN) was located about 1 m away from the sample, from which Debye-Scherrer rings (Fig. 1) were collected. In order to generate 2-theta – Intensity plots, the data was caked into  $10^\circ$  slices centered around the poling direction ( $\Psi = 0^\circ$ ), using Fit2D software [11].

### III. Results and discussion

X-ray diffraction was used to identify the phases present in the calcined powder. The X-ray diffraction patterns were indexed with the reference pattern for tetragonal  $\text{PbZr}_{0.52}\text{Ti}_{0.48}\text{O}_3$  (ICDD: 33-0784). From the XRD pattern (Fig. 2), it is clear that the present calcined PZT powder crystallizes in a tetragonal crystal structure, due to the presence of a single (111) peak and the splitting of the (002)/(200) peaks.

The microstructure of the PZT-ionomer composites with 30 vol.% PZT is shown in the SEM micrographs of a sample fractured at room temperature presented in Fig. 3. All the composites had a pore free nature and PZT particles were uniformly distributed in the polymer matrix. The high resolution image (Fig. 3(b)) shows the good adhesion between polymer matrix and the ceramic particles. As shown in Fig. 3(b) the PZT particles retained their equiaxed morphology after the multiple extrusion process.

By comparing the P-E hysteresis loops, shown in Fig. 4, it is clear that the remnant polarization,  $P_r$ , of the PZT-ionomer composite is far lower than that of the bulk PZT ceramics while the coercive field,  $E_c$ , of the composite is higher than that of the PZT ceramics. For the fully dense PZT ceramic, when the external electric field reaches  $1 \text{ kV mm}^{-1}$ , the hysteresis loop is completely open and saturated, whereas for the composites, when the external field reach as high as  $15 \text{ kV mm}^{-1}$ , the loop only starts to open up but is not saturated. This is mainly due to the presence of a low dielectric, non-piezoelectric polymer layer between the PZT particles, shielding the particles from the applied electric field and significantly lowering the resulting polarization of the PZT particle. A further increment of the applied driving voltage led to electric arcing between the electrodes, making it impossible to apply higher electric fields than  $15 \text{ kV mm}^{-1}$ .

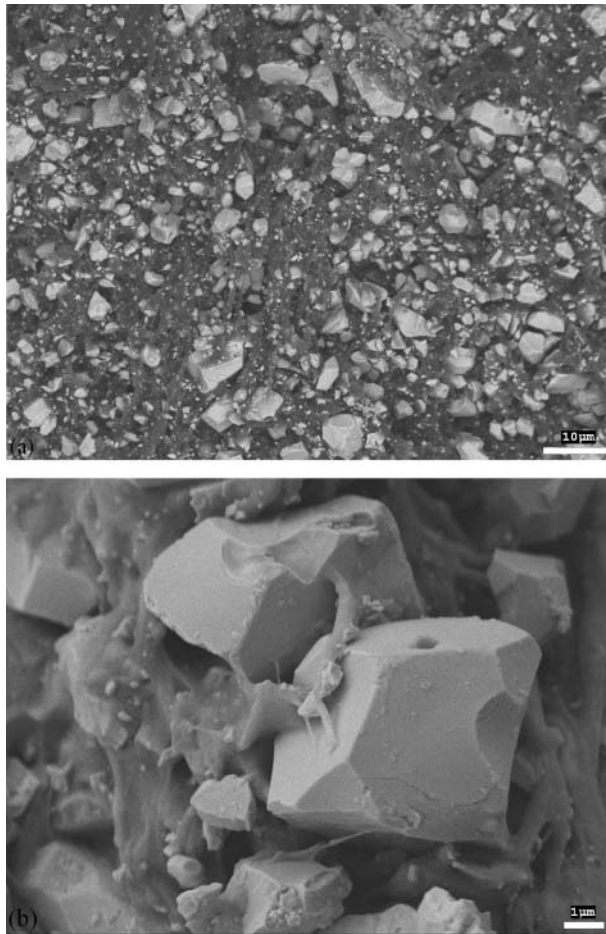


**Figure 3.** SEM micrographs PZT-ionomer composites (a) overview of the cross section and (b) the primary particles.

In contrast to the P-E hysteresis measurements reported above, poling of the composites was carried out at elevated temperatures and the electric field was maintained for a long time (up to 1 hour) to obtain an optimal more-saturated polarization level. In ceramic-polymer composites, the effective electric field experienced by the ceramic phase is controlled by the electrical conductivity and dielectric constant of both ceramic and polymer phases. If the timescale for poling is greater than the dielectric relaxation time constant of each of both phase, it is expected that the distribution of electric field within the PZT and polymer phases is controlled by their electrical resistivities rather than their dielectric properties. Hence we expect to achieve a significantly higher degree of poling of the PZT phase in the poled composites than was evident from the P-E hysteresis measurements, which were conducted over a relatively short timescale.

A detailed study of the piezoelectric and dielectric properties of PZT-ionomer composites has been reported in our previous work showing that poling for longer times at elevated temperatures leads to saturation of the piezoelectric properties, as shown in [Table 1](#). Reversal of  $180^\circ$  ferroelectric domains takes place at the initial stages of poling, while  $90^\circ$  domain

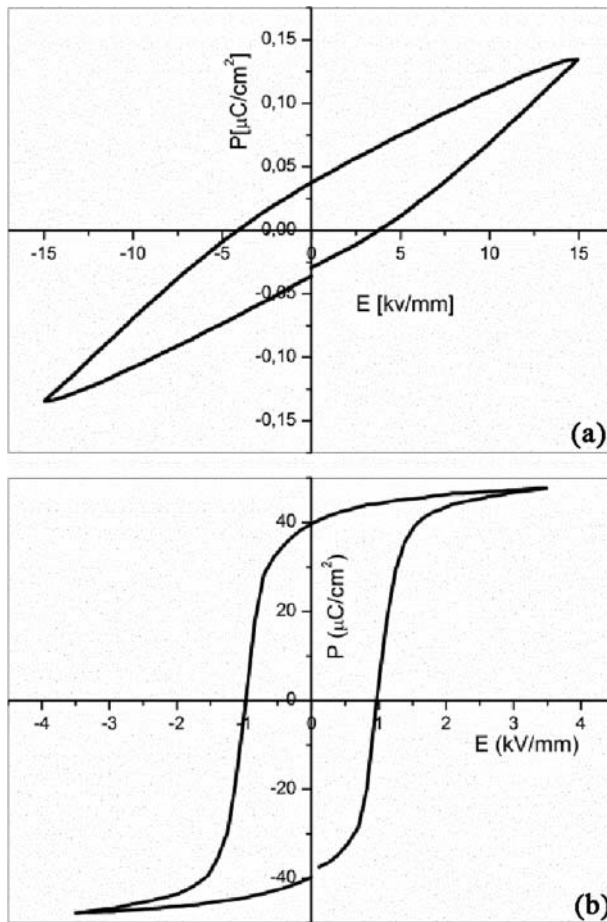


**Figure 4.** P-E hysteresis loops of (a) PZT-ionomer composites and (b) PZT ceramics at room temperature.

reorientation involving local stresses and strains demands longer time poling. The measured piezoelectric charge coefficient of the PZT-ionomer composites is in agreement with the values predicted by Yamada's model [6]. In this model, it is assumed that the PZT phase is completely poled and hence the poling efficiency factor, ' $\alpha$ ' is taken as 1. The actual state of poling was determined using synchrotron X-ray diffraction results.

The high energy synchrotron XRD patterns of PZT-ionomer composites in the unpoled and poled conditions are compared in Fig. 5, for an azimuthal angle  $\psi = 0^\circ$ . The

**Table 1.** Piezoelectric charge coefficients of the PZT-ionomer composites, obtained after poling under an electric field of 15 kV mm<sup>-1</sup> with various temperatures and time [6].

Poling condition Temperature (°C)	Time (hrs)	$d_{33}$ (pC.N <sup>-1</sup> )
25	2	2.8
60	0.5	3.0
60	1	4.5
80	1	4.5

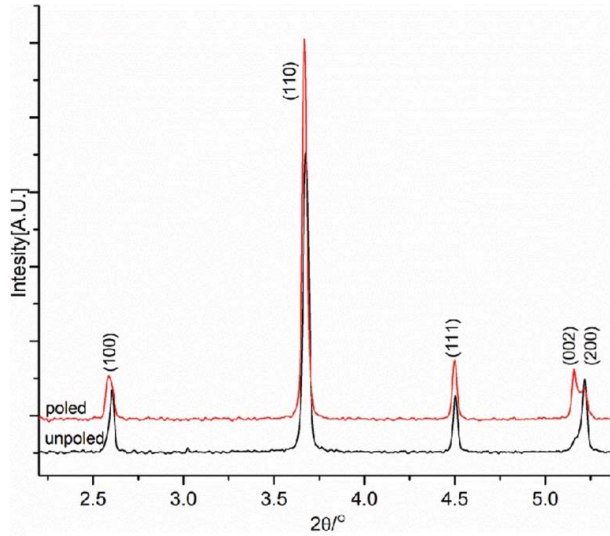


**Figure 5.** Integrated high energy synchrotron XRD patterns of PZT-ionomer composite, for  $\psi = 0^\circ$ .

crystallographic analysis of the phases present in the composite shows that the PZT powder is phase pure and consistent with a tetragonal PZT perovskite structure, as reported previously [12]. It is known that stress due to non  $180^\circ$  domain reorientation and inter-granular strains in polycrystalline ferroelectrics can lead to changes in the intensities and positions of specific diffraction peaks [11, 13–15]. The structural changes of the PZT particles inside the polymer matrix were subsequently investigated by analysing and comparing the diffraction peak profiles obtained for the unpoled and poled composites.

Fig. 6 illustrates schematically the evolution of domain reorientation and overall strain developed during the poling process. The family of grains or particles having their  $\{001\}$  planes oriented perpendicular to the applied electric field direction ( $\psi = 0^\circ$ ) experience a tensile (positive) elongation in this direction and a compressive (negative) elongation in the transverse direction ( $\psi = 90^\circ$ ) due to the combination of the intrinsic piezoelectric effect and extrinsic non- $180^\circ$  ferroelectric domain switching during poling. Although the piezoelectric strain disappears when the electric field is removed, the transformation strain due to domain switching remains as a result of the non-zero remnant polarization. In contrast,

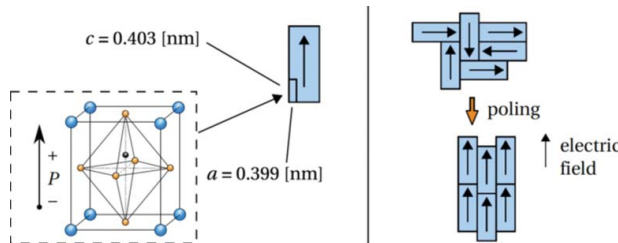


**Figure 6.** Schematic representation of strain development due to ferroelectric domain reorientation during the poling process [16].

ferroelectric domain switching within a {111}-oriented grain causes zero elongation along the poling direction, provided that there is no significant elastic constraint. Therefore, the {111} grain family can serve as a convenient sensor to detect the influence of elastic constraint and the associated residual stress due to poling [12].

The lattice strain during poling results in a shift in the d-values as determined from the diffraction pattern and can be calculated by the following equation:

$$\varepsilon_{hkl} = \frac{d_{hkl(\text{poled})} - d_{hkl(\text{unpoled})}}{d_{hkl(\text{unpoled})}} \quad (1)$$

where  $d_{hkl(\text{poled})}$  and  $d_{hkl(\text{unpoled})}$  are the lattice spacing of a given (hkl) plane in the poled and unpoled conditions respectively [14]. The {111} diffraction peaks were used to calculate the lattice strain since the {111}-oriented grains respond to tensile or compressive inter-granular stresses caused by ferroelectric domain reorientation within neighbouring grains [14]. Changes in the {111} peak position as a function of the azimuthal angle  $\psi$  for the poled composite are illustrated in Fig. 7. It is evident that the {111} peak shifts to lower angles and hence larger d-spacings as  $\psi$  reduces, indicating the presence of a tensile residual stress along the poling direction ( $\psi = 0^\circ$ ) in the PZT particles. In contrast, for the unpoled composite (not shown) it was found that the {111} peak positions showed no systematic change with  $\psi$ , confirming that the PZT particles in the unpoled composite were not subjected to any significant residual stresses.

The positions of the {111} diffraction peaks were determined by fitting the peak profiles to a pseudo-Voigt function and hence calculating the lattice spacings using the Bragg equation. Subsequently the lattice strain,  $\varepsilon_{\{111\}}$ , was calculated according to equation (1). The results of these calculations are presented in Fig. 8. It is evident that the  $\varepsilon_{\{111\}}$  values for the unpoled composite were essentially independent of  $\psi$  and were scattered about the zero level. For the poled composite, an approximately linear relationship was obtained between  $\varepsilon_{\{111\}}$  and  $\cos^2\psi$ , similar to that observed in poled tetragonal PZT ceramics [12]. The

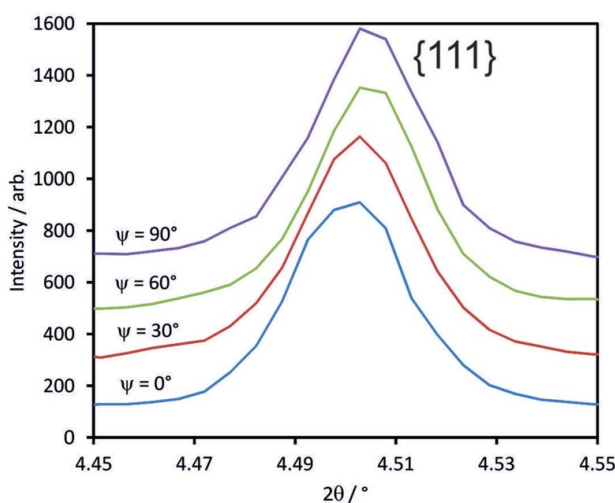


**Figure 7.** Changes in {111} peak position as a function of azimuthal angle  $\Psi$  for poled composite.



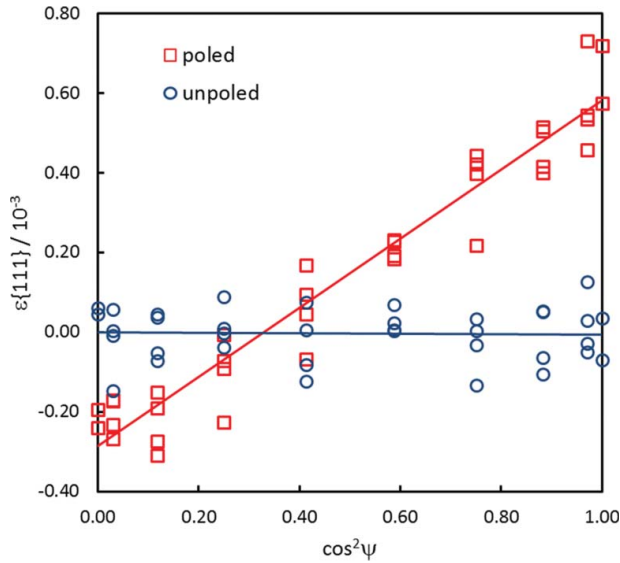


**Figure 8.** Lattice strain  $\varepsilon\{111\} - \cos^2 \Psi$  plots for unpoled and poled composites.

maximum strain of approximately 0.6% is lower than the value of 1% reported previously for a poled tetragonal PZT ceramic, but it does indicate that the PZT particles in the composite are subject to a significant level of elastic constraint and that this gives rise to residual stresses during poling. This result was unexpected, since it was anticipated that the difference between the elastic moduli of the ceramic and polymer phases should result in a relatively free (unconstrained) state for the PZT particles. This behavior could possibly be caused by elastic particle-particle interactions, since the volume fraction of the ceramic phase is relatively high, or the presence of hard particle agglomerates. Further work is required to establish whether any of these mechanisms could give rise to the observed level of residual stress in the poled composite.

The changes in the  $\{002\}$  peak profiles of the poled composite as a function of the azimuthal angle,  $\psi$ , are presented in Fig. 9. Poling of a polycrystalline ferroelectric material is achieved by domain reorientation within the grains and thus by a local change of domain fractions. This reorientation of domains towards the direction of the applied electric field ( $\psi = 0^\circ$ ) is clearly reflected in the relative intensities of the (002) and (200) diffraction peaks. More specifically, the intensity of the (002) peak increases while that of the (200) peak decreases with decreasing  $\psi$ . This indicates that a greater proportion of  $c$ -axis domains, with their spontaneous polarisation directed along  $\langle 001 \rangle$ , are evident in the XRD pattern obtained at  $\psi = 0^\circ$ , while the opposite occurs at  $\psi = 90^\circ$ .

The volume fraction of  $c$ -axis domains oriented along any given direction can be calculated from the intensities of the (002) and (200) diffraction peaks as

$$v_{002} = \frac{\frac{I_{002}}{I_{002}}}{\frac{I_{002}}{I_{002}} + 2 \frac{I_{200}}{I_{200}}} \quad (2)$$

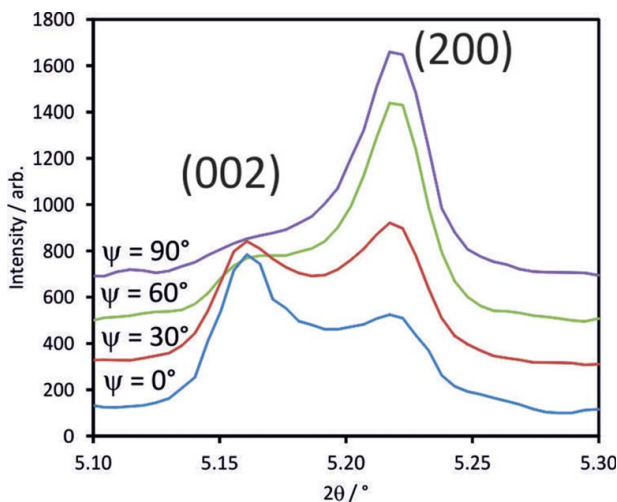


**Figure 9.** Changes in {200} peak profiles as a function of azimuthal angle,  $\Psi$ , for the poled composite.

where  $I_{hkl}$  and  $I'_{hkl}$  denote the integrated area of a given plane for the poled (oriented) and unpoled (randomly oriented) conditions respectively [15]. The value of  $\nu_{002}$  should be equal to  $1/3$  in the unpoled state and  $1$  in the fully poled state, for  $\psi = 0^\circ$ .

The dependence of  $\nu_{002}$  on  $\psi$  for both the unpoled and poled composites is illustrated in Fig. 10. It is evident that the value of  $\nu_{002}$  for the unpoled composite is scattered around the fixed value of  $1/3$ , as defined by equation (2). In contrast,  $\nu_{002}$  for the poled composite exhibits a linear dependence on  $\cos^2\psi$ , which reflects the macroscopic strain state induced by

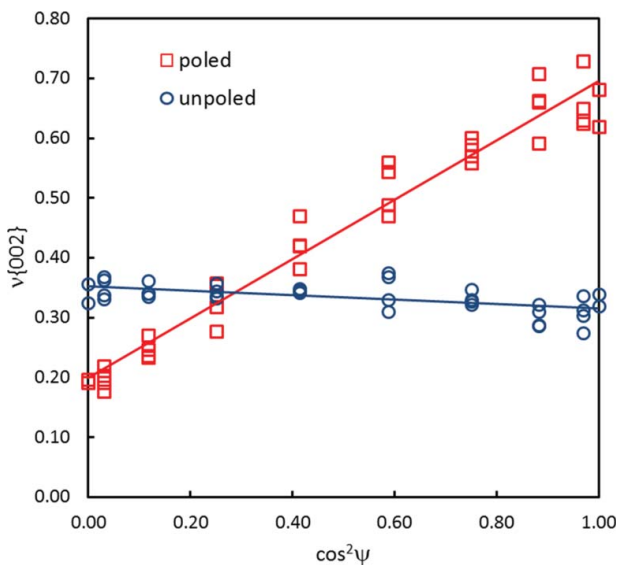


**Figure 10.** Variation in fraction of c-axis oriented domains,  $\nu\{002\}$ , as a function of  $\cos^2 \Psi$  for unpoled and poled composites.

poling and leads to a similar relationship for the lattice strain  $\varepsilon\{111\}$  through the occurrence of residual stress [12]. The maximum value of  $\nu_{002}$ , obtained for  $\psi = 0^\circ$ , was approximately 0.70; this is considerably larger than the value of approximately 0.47 observed previously in a tetragonal PZT ceramic by Hall [12].

Jones employed a different indicator,  $\eta_{002}$ , to describe the crystallographic texture in poled PZT ceramics<sup>15</sup>. This texture indicator was used to quantify the volume fraction of switched domains and is related to  $\nu_{002}$  by

$$\eta_{002} = \nu_{002} - \frac{1}{3} \quad (3)$$

It was reported that  $\eta_{002}$  values for poled tetragonal PZT ceramics in the literature varied from 0.13 to 0.46, corresponding to  $\nu_{002}$  values in the range 0.46 to 0.79 [15]. In comparison with these values, it is evident that the degree of poling achieved for the PZT-ionomer composites in the present study is relatively high, in accordance with the bulk piezoceramic results. In the present case, the 2.3  $\mu\text{m}$  size PZT particles are big enough to accommodate the domains and the poling conditions employed were adequate to materialize the maximum piezoelectric properties out of the composite.

#### IV. Conclusions

The poling behaviour of the tetragonal PZT particles in a Zn based ionomer polymer matrix has been analysed using high energy synchrotron X-ray diffraction. The reorientation of ferroelectric domains during poling was quantified in terms of the parameter  $\nu_{002}$ , which represents the volume fraction of c-axis domains oriented in any given direction,  $\psi$ , relative to that of the applied electric field. It was shown that the highest value of  $\nu_{002}$ , equal to 0.70, was obtained for domains oriented along the poling direction ( $\psi = 0^\circ$ ), demonstrating that a relatively high degree of poling could be achieved using this polymer matrix with a moderate electrical conduction, a high field and a long poling time. An approximately linear  $\nu_{002} - \cos^2\psi$  relationship was observed, in agreement with previous studies of poled tetragonal PZT ceramics. Unexpectedly, it was also found that the lattice strain,  $\varepsilon\{111\}$ , exhibited a linear dependence on  $\cos^2\psi$ , reaching a maximum value around  $0.6 \times 10^{-3}$  for  $\psi = 0^\circ$ . This result indicates that the PZT particles in the composite are subject to considerable elastic constraint, even though the elastic moduli of the two constituent phases differ by several orders of magnitude. Clearly the strain evolution is due to domain reorientation and not so much due to mechanical constraints of the polymer matrix surrounding the particle.

#### Acknowledgments

The authors are grateful to Morgan Electro Ceramics for providing the PZT507 powder and ceramics used in this research. The authors gratefully acknowledge the technical support provided by Diamond Light Source Ltd, UK for the synchrotron XRD experiment.

#### Funding

This work was financially supported by the Smartmix funding program (Grant No. SMVA06071), as part of the program "Smart systems based on integrated Piezo."

## References

1. A. J. Moulson and J. M. Herbert, *Electroceramics*. John Wiley & Sons. Ltd, U.S.A., 2003
2. B. Jaffe, W. R. Cook Jr, and H. Jaffe, *Piezoelectric Ceramics*. Academic Press London and New York 1971.
3. R. E. Newnham, D. P. Skinner and L. E. Cross, “connectivity and Piezoelectric-pyroelectric composites,” *Mater. Res. Bull.* **13**(5), 525–36 (1978).
4. G. Sa-Gong, A. Safari, S. Jang, and R. Newnham, “Poling of Flexible piezoelectric composite,” *Ferroelectr. Lett. Sect.*, **5**, 131–42 (1986).
5. D. Waller, T. Iqbal, and A. Safari, “Poling of Lead Zirconate Titanate and Flexible Piezoelectric Composites by the Corona Discharge Technique,” *J. Am. Ceram. Soc.*, **72**, 322–4 (1989).
6. N. K. James, U. Lafont, S. van de Zwaag and W.A. Groen, “Piezoelectric and mechanical properties of fatigue resistant self-healing PZT-ionomer composites,” *Smart Mater. Struct.*, **23**(5), 055001 (2014).
7. A. Pramanick, D. Damjanovic, J. E. Daniels, J. C. Nino, and J. L. Jones, “Subcoerceive cyclic electrical loading of lead Zirconate titanate ceramics I: nonlinearities and losses in the converse piezoelectric effect,” *J. Am. Ceram. Soc.*, **94**, 2291–9 (2011).
8. J. L. Jones, B. J. Iverson, and K. J. Bowman, “Texture and Anisotropy of Polycrystalline Piezoelectrics,” *J. Am. Ceram. Soc.*, **90**(8), 2297–314 (2007).
9. R. Guo, L. E. Cross, S. E. Park, B. Noheda, D. E. Cox, and G. Shirane, “Origin of the High Piezoelectric Response in  $\text{PbZr}_{(1-x)}\text{Ti}_x\text{O}_3$ ,” *Phys. Rev. Lett.*, **84**[23], 5423–6 (2000).
10. D. A. van den Ende, W. A. Groen, and S. van der Zwaag, “The effect of calcining temperature on the properties of 0/3 piezoelectric composites of PZT and a liquid crystalline thermosetting polymer,” *J. Electroceram.* **27**(1), 13–19 (2011).
11. A. Hammersley, S. Svensson, M. Hanfland, A. Fitch, and D. Hausermann, “Two-dimensional detector software: from real detector to idealised image or two-theta scan,” *International Journal of High Pressure Research*, **14**(4 6) 235–48 (1996).
12. D.A. Hall, A. Steuwer, B. Cherdhirunkorn, P.J. Withers and T. Mori, “Micromechanics of residual stress and texture development due to poling in polycrystalline ferroelectric ceramics”, *J. Mech. Phys. Solids* **53**, 249–260 (2005).
13. J. L. Jones, A. Pramanick, J. C. Nino, S. Maziar Motahari, E. Üstündag, M. R. Daymond, and E. C. Oliver, “Time resolved and orientation dependent electric-field induced strains in lead zirconate titanate ceramics,” *Appl. Phys. Lett.*, **90**, 172909–3 (2007).
14. A. Pramanick and J. L. Jones, “Measurement of Structural changes in Tetragonal PZT ceramics under static and cyclic electric fields using a laboratory X-ray diffractometer,” *IEEE Trans. Ultrason., Ferroelectr., Freq. Control*, **56**(8), 1546–54 (2009).
15. J. L. Jones, E. B. Slamovich, and K. J. Bowman, “Domain texture distributions in tetragonal lead zirconate titanate by x-ray and neutron diffraction,” *J. Appl. Phys.*, **97**, 034113–6 (2005).
16. J. Holterman and W. A. Groen, *An Introduction to piezoelectric materials and applications*. Stichting Applied Piezo, The Netherlands, 2013.